Resonant Spectrum Method to Characterize Piezoelectric Films in Composite Resonators

Yuxing Zhang, Zuoqing Wang, and J. David N. Cheeke, *Senior Member, IEEE*

***Abstract*—In this paper, we present a direct method to characterize a piezoelectric film that is sandwiched with two electrodes and deposited on a substrate to form a four-layer thickness extension mode composite resonator (also known as over-moded resonator). Based on the parallel and series resonant frequency spectra of a composite resonator, the electromechanical coupling factor, the density and the elastic constant of the piezoelectric film can be evaluated directly. Experimental results on samples consisting of ZnO films on fused quartz substrates with different thickness are presented. They show good agreement with theoretical prediction. The mechanical effect of the electrode on the method is investigated, and numerical simulation shows that the effect of the electrodes can be properly corrected by the modified formulae presented in this paper. The effect of mechanical loss in piezoelectric film and in substrate on this method also has been investigated. It is proven that the method is insensitive to the losses.**

I. Introduction

Piezoelectric thin films have been widely used in high frequency bulk acoustic wave (BAW) and surface acoustic wave (SAW) devices, such as filters, resonators, actuators, and sensors. For self-supported, single piezoelectric films, various measurement techniques have been developed to evaluate the acoustic properties of these films. However, for some piezoelectric ceramic films (e.g., sol-gel PZT films on metal substrate [1]) and for very high frequency acoustic wave devices (e.g., zinc oxide films on fused quartz [2], [3] and AlN films on silicon [4]), the films are not self-supported and the film properties depend on the substrates. Therefore, the methods recommended by the IEEE standard [5] are not available.

In the case of thin films deposited on very thick substrates, which are used as high frequency transducers, Bahr and Court [6] developed a method to determine the coupling coefficient from measuring the transducer input admittance. By pulse measurements, an infinite long delay line is imitated, and thus the propagation characteristics of the acoustic wave in the substrate does not affect the measured values of the input admittance. The electromechanical coupling coefficient k_t^2 was determined by data-fitting the input admittance curve (versus frequency). Meitzler and Sittig [7] improved the method by taking the effects of the electrode and the interconnection layers into account. Because the value of k_t^2 is evaluated from the magnitude of the input admittance, which depends on all the electrical factors, a complicated measurement system and very accurate calibration of the system are necessary.

In the case of a piezoelectric film deposited on a thin substrate to form a thickness extension mode composite (over-moded) resonator, Hickernell [3] and Naik *et al.* [4] introduced methods to extract the k_t^2 value by fitting the electric input impedance and admittance data with the equivalent circuit analysis results on multimode resonance of a composite resonator.

We previously reported a direct method to characterize a piezoelectric film coated on an isotropic substrate to form a two-layer composite resonator [8], [9]. By knowing the resonant spectra of a composite resonator, three parameters of the piezoelectric film (i.e., the electromechanical coupling coefficient, the elastic constant, and the density) could be determined. The validity of this method was demonstrated with simulations when electrodes were ignored. For the high frequency devices, however, the electrode effect cannot necessarily be ignored.

In this paper, the resonant spectrum method is extended to the case in which the electrodes are taken into account. A set of explicit formulae that forms the foundation of the method are first presented, followed by the experimental results on high frequency ZnO/fused quartz composite resonators. The validation and the accuracy of the method are proven by numerical simulation in Section IV. The impact of the mechanical effect of electrodes is discussed and the improvement of the method for the electrode effect is demonstrated in Section V. Because the mechanical losses of the materials play an important role on the electric impedance of high-frequency resonators, from which the resonant frequencies are determined, the effect of the mechanical losses on the resonant spectrum method is investigated by numerical simulation in Section VI. In all the simulations, the experimentally measured data for the ZnO thin film (obtained from Section III) are taken as the standard parameters; other parameters are taken from literature. A detailed derivation of the related formulae is presented in the Appendix.

II. The Resonant Spectrum Method

The resonant spectrum method is based on two groups of approximate formulae, which are derived from the elec-

Manuscript received January 10, 2002; accepted October 1, 2002. This work was supported by the Natural Sciences and Engineering Research Council of Canada (NSERC).

Y. Zhang is with the Wireless Technology Lab, Nortel Networks, Ottawa, Ontario K2H 8E9, Canada (e-mail: zhangy@nortelnetworks.com).

Z. Wang is with the TXC Corporation, Tao-Yuan County, Taiwan, R. O. China.

J. D. N. Cheeke is with the Physics Department, Concordia University, Montreal, Quebec H3H 1M8, Canada.

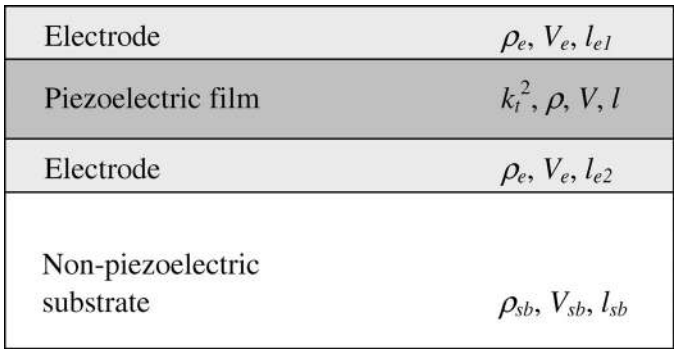

Fig. 1. A typical four-layer composite resonator, with the definitions of the material parameters and dimensions.

tric input impedance expression of a four-layer composite resonator. A composite resonator has multiple resonances, determined mainly by the acoustic properties of the materials and the thickness of the four layers. Three parameters (i.e., longitudinal velocity V, density ρ, and electromechanical coupling coefficient k_t^2) of the piezoelectric film can be determined directly from the parallel and series resonant spectra of a composite resonator. The detailed derivation of the formulae will be given in the Appendix. In this section only the results are presented.

The electric input impedance of a four-layer thickness extension mode composite resonator, as shown in Fig. 1, is:

$$Z_{in} = \frac{1}{j\omega C_0}\left[1 - \frac{k_t^2}{\gamma}\frac{(z_1+z_2)\sin\gamma + j2(1-\cos\gamma)}{(z_1+z_2)\cos\gamma + j(1+z_1z_2)\sin\gamma}\right], \quad (1)$$

where $C_0 = \varepsilon_{33}^S S/l$ is the static capacitance of the resonator, S is the area of the electrodes, ε_{33}^S and l are the permittivity and thickness of the piezoelectric layer; k_t^2 is the electromechanical coupling coefficient of the piezoelectric layer; $\gamma = \omega l/V$ is the phase delay of the longitudinal acoustic wave with velocity V in the piezoelectric layer, ω is the angular frequency; z_1 and z_2 are the acoustic loading impedances on both sides of the piezoelectric layer normalized to $Z_0 = S\rho V$, the acoustic impedance of the piezoelectric layer, ρ is the density of the piezoelectric layer.

Fig. 2 shows the electric input impedance of a resonator consisting of a PZT film deposited on a stainless steel plate. The parameters used are listed as sample III in Table I. In the calculation, an arbitrary small imaginary part (0.1%) is added to the velocities for both the film and the substrate to avoid singularities.

It is shown in Fig. 2 that the impedance response has a global hyperbolic decrease, which is determined by the static capacitance C_0; and, in the frequency region corresponding to the fundamental mode of the piezoelectric film, there is a series of resonant peaks, each peak corresponds to a resonant mode of the composite resonator. The static capacitance C_0 is only related with the hyperbolic decrease of the impedance response, not with the resonant frequencies. Contrarily, k_t^2 should be related only with the resonant frequencies as it is in the single piezoelectric plate

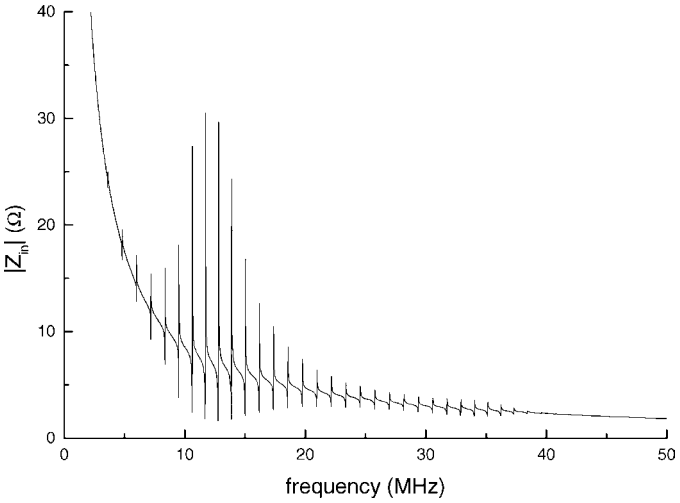

Fig. 2. The simulated electric impedance of a PZT/stainless steel composite resonator as a function of frequency. The curve clearly shows the hyperbolic decrease due to the static capacitance and the peaks due to multiple resonances in the substrate.

case. In the derivation of the method, we followed a similar procedure as in the single piezoelectric plate case to derive the parallel and series resonance frequency equations from (1). From the resonant frequency equations, we derived the formulae that are the principles of the proposed resonant spectrum method.

By definition in the IEEE standard [5], the parallel resonant frequency corresponds to the maximum resistance, which is the real part of Z_{in}. It can be derived from (1) by setting the denominator to zero and is given by:

$$(z_1+z_2)\cos\gamma + j(1+z_1z_2)\sin\gamma = 0. \quad (2)$$

The series resonant frequency, which corresponds to the maximum of the conductance, can be derived from (1) by setting the numerator to zero and is given by:

$$(z_1+z_2)\cos\gamma + j(1+z_1z_2)\sin\gamma - \frac{k_t^2}{\gamma}(z_1+z_2)\sin\gamma + j2(1-\cos\gamma) = 0. \quad (3)$$

It will be seen in the Appendix that z_1 and z_2 are purely imaginary functions if the material parameters are real, so (2) and (3) are not complex equations.

For a multimode composite resonator, by defining the spacing of the parallel resonant frequencies (SPRF)

$$\Delta f_p(m) = f_p(m+1) - f_p(m), \quad (4)$$

we derived two approximate formulae that relate the longitudinal velocity V and the density ρ of the piezoelectric layer with two characteristic values of the SPRF, Δf_N and Δf_T, which can be obtained from the SPRF distribution versus the resonant mode order m.

The normal regions are the areas in which γ is close to an integer multiplication of π. At the center of the first normal region (i.e., $\gamma \approx \pi$), the SPRF is given by:

$$\Delta f_N = \Delta f_0 \left(1 + \frac{\rho_{e1}l_{e1} + \rho_{e2}l_{e2} + \rho l}{\rho_{sb}l_{sb}}\right)^{-1}, \quad (5)$$

TABLE I
THE PARAMETERS OF COMPOSITE RESONATORS USED IN SIMULATION.

		Piezoelectric film				Substrate				Electrodes			
Sample	Material	ρ (kg/m^3)	V (m/s)	k_t^2 (%)	l (μm)	ρ_{sb} (kg/m^3)	V_{sb} (m/s)	l_{sb} (μm)	z_{sb}	ρ_e (kg/m^3)	V_e (m/s)	l_e (μm)	R
I	ZnO/fused quartz	5665.8	6063.1	7.27	4.8	2200	5973.4	1536.5	0.38	2695	6418	0.4	306.7
II	ZnO/fused quartz	5525.3	6135.9	8.02	5.3	2200	5973.4	2370.3	0.39	2695	6418	0.4	435.4
III	PZT/stainless steel	7000.0	2400	4.0	50	7800	5900	2400	2.74			0	19.5

where $\Delta f_0 = V_{sb}/2l_{sb}$ is the SPRF of the bare substrate plate so it is a constant; ρ_{sb}, ρ_{e1}, and ρ_{e2} are the densities of the substrate, the top and the middle electrodes, respectively; l_{sb}, l_{e1}, and l_{e2} are the thicknesses of the substrate, the top and the middle electrodes, respectively.

For the case in which the acoustic impedance of the piezoelectric layer is greater than that of the substrate referred as soft substrate (e.g., ZnO film on quartz substrate), Δf_N corresponds to the first minimum of the SPRF. In the case in which the acoustic impedance of the piezoelectric layer is less than that of the substrate, referred to as hard substrate (e.g., PZT on stainless steel substrate), Δf_N corresponds to the first maximum of the SPRF.

The transition regions are the areas in which γ is close to a half integer multiplication of π. At the center of the first transition region (i.e., $\gamma \approx \pi/2$), the SPRF is given by:

$$\Delta f_T = \Delta f_0 \left(1 + \frac{\rho_{sb}V_{sb}^2}{\rho V^2}\frac{l}{l_{sb}} + \frac{\rho_{sb}V_{sb}^2}{\rho_{e2}V_{e2}^2}\frac{l_{e2}}{l_{sb}} + \frac{\rho_{sb}\rho_{e1}V_{sb}^2}{\rho^2 V^2}\frac{l_{e1}}{l_{sb}}\right)^{-1}, \quad (6)$$

where V, V_{sb}, V_{e1}, and V_{e2} are the velocities of the piezoelectric layer, substrate, and top and middle electrodes, respectively.

When the acoustic impedance of the piezoelectric layer is greater than that of the substrate, Δf_T corresponds to the first maximum of the SPRF. In the other case Δf_T corresponds to the first minimum of the SPRF.

It is shown in (5) and (6) that the density ρ and the longitudinal velocity V of the piezoelectric layer can be evaluated by obtaining the two characteristic values, Δf_N and Δf_T, from the SPRF distribution and by knowing the thickness of the piezoelectric film and other parameters of the electrodes and the substrate. The elastic constant c_{33}^D then is given by the formula $c_{33}^D = \rho V^2$. Of course, these two formulae can be used to evaluate other parameters if ρ and/or V are known.

In analogy to the formula for the coupling coefficient of a single-layer piezoelectric resonator when the coupling coefficient is small [5]:

$$k_{t,\text{single}}^2 \approx \frac{\pi^2}{4}\frac{f_s}{f_p}\left(1 - \frac{f_s}{f_p}\right), \quad (7)$$

we introduce an effective coupling coefficient $k_{\text{eff}}^2(m)$, which indicates the electromechanical coupling intensity of a specific resonant mode of a composite resonator:

$$k_{\text{eff}}^2(m) = \frac{\pi^2}{4}\frac{f_s(m)}{f_p(m)}\left(1 - \frac{f_s(m)}{f_p(m)}\right), \quad (8)$$

where $f_p(m)$, $f_s(m)$ are the m-order parallel and series resonant frequencies, respectively. From the series resonant frequency determination (3), we derived the relationship between k_t^2 and $k_{\text{eff}}^2(m)$ as follows.

At the first normal region k_t^2 is given by:

$$k_t^2 = \frac{(1 + m_N z_{sb})^2}{\left(1 + \frac{\rho_{e1}l_{e1} + \rho_{e2}l_{e2} + \rho_{sb}l_{sb}}{\rho l}\right)} k_{\text{eff}}^2(m_N + 1), \quad (9)$$

where $z_{sb} = Z_{sb}/Z_0$ is the normalized acoustic impedance of the substrate, $Z_{sb} = S\rho_{sb}V_{sb}$, $(m_N + 1)$ is the resonant mode order at the center of the first normal region.

At the first transition region, k_t^2 is given by:

$$k_t^2 = \frac{\left[(2m_T + 1)/z_{sb} + 1\right]^2}{1 + \frac{\rho V^2/l}{\rho_{sb}V_{sb}^2/l_{sb}} + \frac{\rho V^2/l}{\rho_{e2}V_{e2}^2/l_{e2}} + \frac{\rho_{e1}l_{e1}}{\rho l}} \frac{k_{\text{eff}}^2(m_T + 1)}{\Gamma}, \quad (10)$$

where $(m_T + 1)$ is the resonant mode order at the center of the first transition region. Γ is a correction factor, which is caused by the difference between the $(m_T + 1)$ order series resonant frequency and the center of the first transition region. Γ is given by:

$$\Gamma = 1 - 2\rho V\left(1 + \frac{2\pi f_s l}{V} - \frac{\pi}{2}\right)\left(\frac{2\pi f_s l}{\rho_{sb}V_{sb}^2} - \frac{(m_T + 1/2)\pi}{\rho_{sb}V_{sb}} + \frac{2\pi f_s l_{e2}}{\rho_{e2}V_{e2}}\right). \quad (11)$$

where f_s is the series resonant frequency at the center of the first transition region.

By knowing the thicknesses, the densities, and the velocities of four layers and by evaluating the $k_{\text{eff}}^2(m)$ value from the experiment/simulation data, k_t^2 can be obtained from (9) or (10). Usually, the maximum value of $k_{\text{eff}}^2(m)$ should be used in the evaluation for the best accuracy. When $Z_0 > Z_{sb}$, the maximum $k_{\text{eff}}^2(m)$ is located in the first normal region and when $Z_0 < Z_{sb}$, the maximum $k_{\text{eff}}^2(m)$ is located in the first transition region.

By introducing the ratio of the half wavelength resonant frequency of the top resonator f_c to the half wavelength resonant frequency of the substrate f_{sb}:

$$R = \frac{f_c}{f_{sb}} = \frac{V\left(l_{sb} + \frac{1}{2}\rho_{e2}l_{e2}/\rho_{sb}\right)}{V_{sb}\left(l + \rho_{e1}l_{e1}/\rho + \frac{1}{2}\rho_{e2}l_{e2}/\rho\right)}, \quad (12)$$

we can get approximate expressions of the mode order at the first normal region and the first transient region:

$$m_N = \text{the nearest integer of } R, \tag{13}$$

$$m_T = \text{the nearest integer of } \left(\frac{R-1}{2}\right). \tag{14}$$

When R is close to an integer or R is so large that the fractional part can be ignored, (9) can be simplified to:

$$k_t^2 = \frac{\rho l\left(\rho l + \rho_{sb} l_{sb} + \rho_{e1} l_{e1} + \rho_{e2} l_{e2}\right)}{\left(\rho l + \rho_{e1} l_{e1} + \frac{1}{2}\rho_{e2} l_{e2}\right)^2} k_{\text{eff}}^2 (m_N + 1). \tag{15}$$

When R is close to an odd integer, or say $(R-1)/2$ is close to an integer, or R is very large, (10) can be simplified to:

$$k_t^2 = \frac{\rho l\left(1 + \frac{\rho_{e1} l_{e1}}{\rho l} + \frac{\rho V^2}{\rho_{sb} V_{sb}^2}\frac{l_{sb}}{l} + \left(\frac{\rho^2 V^2}{\rho_{sb}^2 V_{sb}^2} + 1\right)\frac{\frac{1}{2}\rho_{e2} l_{e2}}{\rho l}\right)}{\rho l + \rho_{e1} l_{e1} + \frac{1}{2}\rho_{e2} l_{e2}} \frac{k_{\text{eff}}^2 (m_T + 1)}{\Gamma}. \tag{16}$$

These simplified equations also have a clear physical interpretation. Eq. (15) shows when the electrodes can be ignored, k_t^2 of the piezoelectric film is the effective coupling factor at the center of the first normal region multiplied by the mass ratio of the whole resonator to the piezoelectric film.

III. Measurement of ZnO/SiO_2 Composite Resonators

In order to demonstrate the feasibility of the resonant spectrum method, some composite resonator samples have been measured. The resonators are composed of ZnO films deposited on fused quartz substrates [10]. The thickness of the ZnO films is about 5 μm and the thicknesses of the quartz substrates are about 62 mil (Sample I) and 92 mil (Sample II). There is a circular ground electrode of aluminum approximately 0.4-μm thick underlying the ZnO film, and there are four small circular electrodes of 0.4 μm aluminum on the top of ZnO film, forming 4 composite resonators (Fig. 3).

The reflection coefficients s_{11} of the resonators were measured with an HP8753D network analyzer (Agilent, Palo Alto, CA) from 100 MHz to 800 MHz. Because the maximum number of measurement points of an HP8753D is only 1601 and we need an ultrahigh resolution resonant spectrum, the whole frequency span of 700 MHz was divided into tens of narrow spans, 10 MHz each for 62-mil thickness samples and 8 MHz each for 92-mil thickness samples. The network analyzer was calibrated only once for 700 MHz span, and an interpolated calibration was used for each measurement. A LabWindow program (National Instruments Corp., Austin, TX) running in a computer was used to control the network analyzer for setting the central frequency and span, running the measurement, and downloading the measured data to the computer. Thus, high-resolution frequency responses for the whole span were acquired.

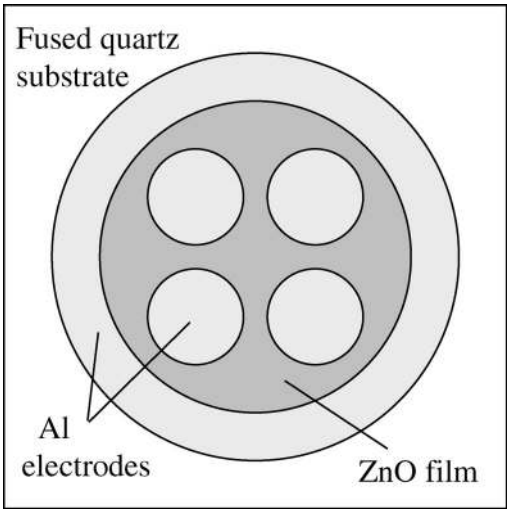

Fig. 3. ZnO/SiO_2 composite resonators used in the experiment. The bottom electrode is common to all four resonators.

After further interpolating the measured data near each resonant peak and then converting s_{11} into impedance Z_{in} and admittance Y_{in}, the parallel and series resonate frequencies of these samples were calculated. Distributions of the SPRF and the $k_{\text{eff}}^2(m)$ of the samples are shown in Figs. 4 and 5, from which the two characteristic values Δf_N, Δf_T and the effective coupling coefficient $k_{\text{eff}}^2(m_N + 1)$ are measured. They are listed in Table II. Here the SPRF and k_{eff}^2 are plotted against frequency, not the mode order as in their definitions. In fact, both are almost identical in the distribution shape and only differ in the horizontal axis by a factor of Δf_0, the SPRF of the bare substrate. It is shown that the data of the SPRF are a little dispersive, and the characteristic values of Δf_N, Δf_T are determined by averaging the measurement data. Even so, the periodic shape of the SPRF distribution is very regular and the results are fairly sure. It is interesting to notice that the data of $k_{\text{eff}}^2(m)$ are very smoothly distributed over a wide frequency range and almost no dispersion. As a result, no data fitting is necessary, and the characteristic value of $k_{\text{eff}}^2(m_N + 1)$ can be evaluated accurately. These experiment results clearly show the practicality of this method.

The density ρ, the longitudinal velocity V (then the elastic constant c_{33}^D), and the electromechanical coupling coefficients k_t^2 of the ZnO film were then calculated by using the resonant spectrum method (5), (6), and (9). They are listed in Table II. The data of the thickness and the parameters of the fused quartz substrate and aluminum electrodes [10], [11] are given in Table I.

IV. Validity and Accuracy of the Resonant Spectrum Method

Since the ZnO film parameters are process related, there are no standard values to compare with the results we got from the experiment. We will investigate the valid-

TABLE II

CHARACTERISTIC VALUES AND PARAMETERS DETERMINED BY EXPERIMENT ON ZNO/FUSED QUARTZ COMPOSITE RESONATORS.

	Experiment			Parameters deduced from experiment				
Sample	Δf_N (MHz)	Δf_T (MHz)	$k^2_{\text{eff}}(m_N+1)$ (%)	m_N+1	ρ (kg/m^3)	c^D_{33} (10^{10}N/m^2)	V (m/s)	k^2_t (%)
1	1.9271	1.9411	0.065	309	5665.8	20.83	6063.1	7.27
2	1.2525	1.2588	0.050	437	5525.3	20.80	6135.9	8.02

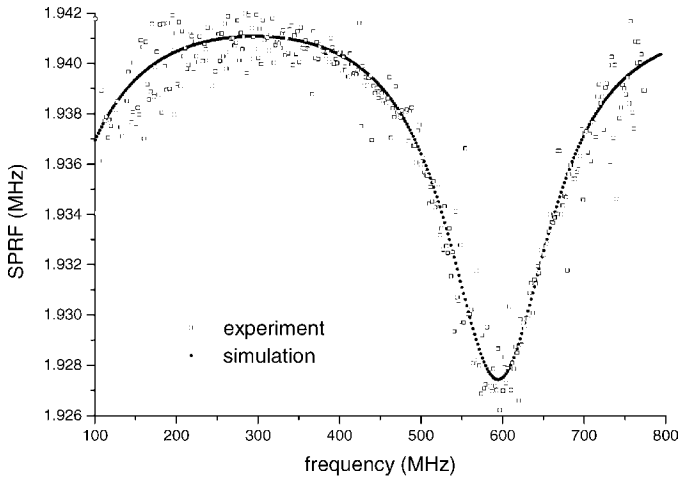

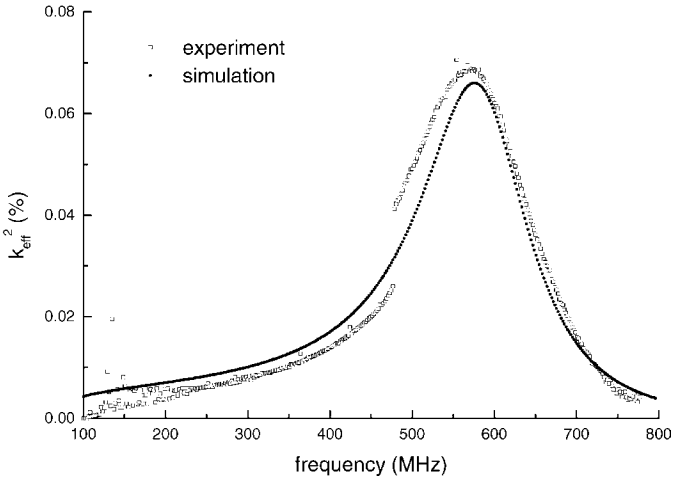

Fig. 4. SPRF (top) and k^2_{eff} (bottom) distribution of Sample I (62 mil ZnO/fused quartz resonator).

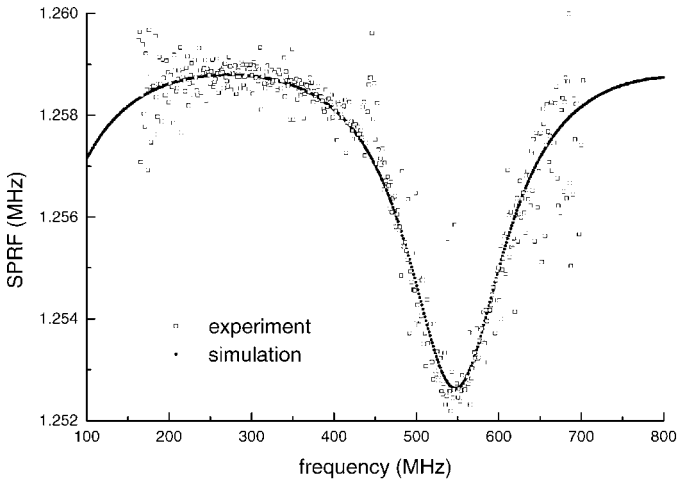

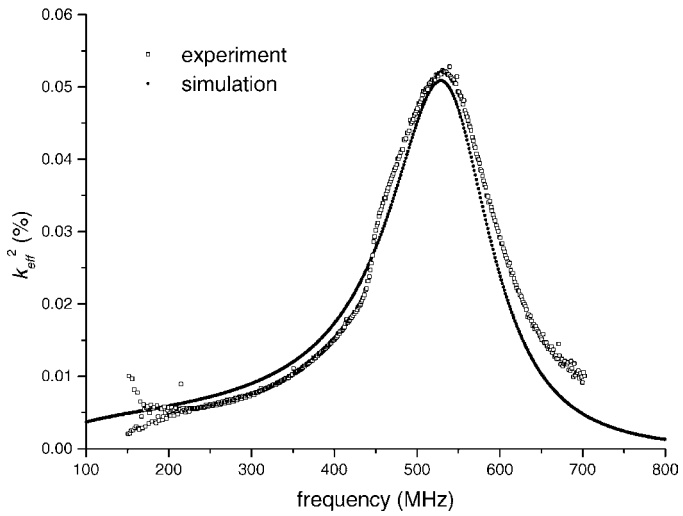

Fig. 5. SPRF (top) and k^2_{eff} (bottom) distribution of Sample II (92 mil ZnO/fused quartz resonator).

ity and accuracy of the method by numerical simulation. Three examples are simulated. The first two are the samples discussed in last section (i.e., ZnO film on fused quartz substrate), which represent the case in which the acoustic impedance of the piezoelectric layer is greater than that of the substrate. The values of the velocity, the density, and the coupling coefficient of the ZnO films are the data determined by experiment in the last section. In the simulation they are used as the input parameters. The third sample is a porous PZT film on a stainless steel plate [1], which represents the case in which the acoustic impedance of the piezoelectric layer is less than that of the substrate. The parameters used in the simulation are listed in Table I.

The parallel and series resonant frequencies of these composite resonators are calculated by solving the maximums and minimums of the resistance from (1). The distribution of the SPRF and $k^2_{\text{eff}}(m)$ of Sample I and Sample II are shown in Figs. 4 and 5 by solid dots. For Sample III, they are shown in Fig. 6. The simulated characteristic values of Δf_N, Δf_T, and $k^2_{\text{eff}}(m_N+1)$ are obtained from these figures. Using the equations of the resonant spec-

TABLE III
SIMULATION RESULTS ON THE SAMPLES IN TABLE I.

Sample	ρ (kg/m^3)	error	c_{33}^D (10^{10}N/m^2)	error	V (m/s)	error	k_t^2 (%)	error
I	5544.2	−2.1%	20.67	−0.8%	6106.1	0.7%	7.05	−3.0%
II	5422.5	−1.9%	20.63	−0.8%	6167.9	0.5%	7.75	−3.4%
III	7011.8	0.2%	4.10	1.6%	2419.2	0.8%	3.98	−0.4%

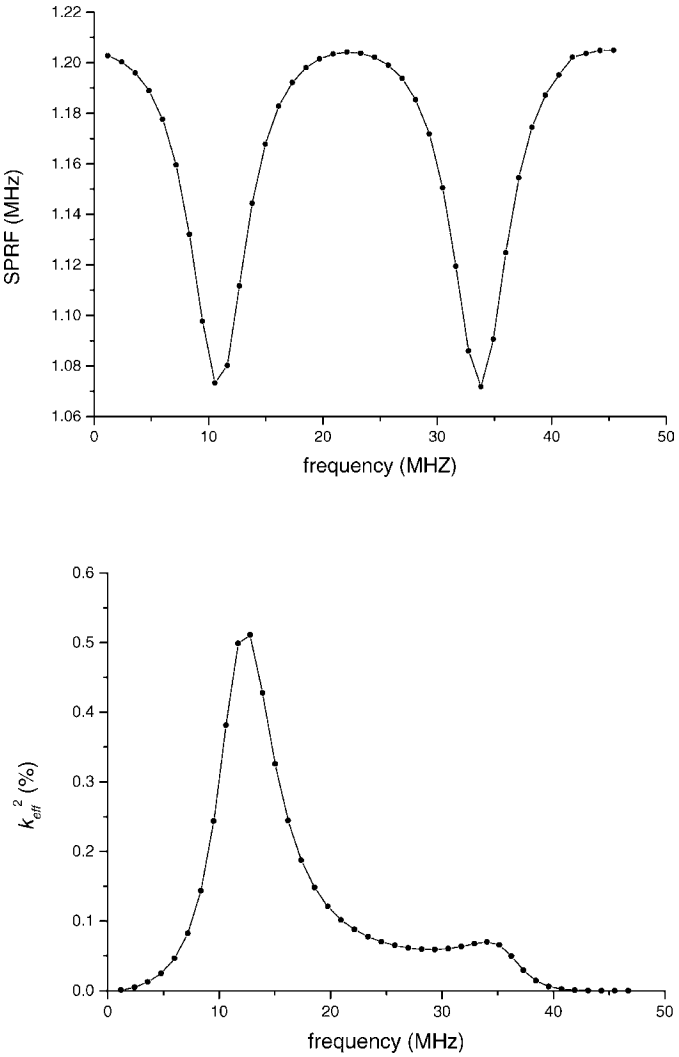

Fig. 6. SPRF (top) and k_{eff}^2 (bottom) distribution of Sample III (PZT/stainless steel resonator).

trum method in Section II and the material parameters in Table I, we obtained the simulation output of three parameters of the piezoelectric films. The results are listed in Table III. The errors listed are with reference to the input data shown in Table I. Small imaginary parts are introduced into the velocities of both the piezoelectric film and the substrate to avoid singularities. The imaginary parts of the velocities have little effect on the distribution of the SPRF and the effective coupling coefficients. This will be discussed in Section V.

It is shown in Table III and the input data given in Table I that the difference between the output values and input values are within 3.5% for all three parameters (and c_{33}^D as well). Assuming the data evaluated from the experiment (given in Table II and listed in Table I as the input parameters) are the "true" values for Sample I and Sample II, the determined values by this method are accurate to 3.5% for the samples used here. For such high frequency devices, a few percent errors are quite acceptable.

V. Effect of the Electrodes

In our previous work [8], the mechanical effect of electrode was ignored. In other words, the thickness of the electrodes was taken to be zero. In this paper, we have taken the electrodes into account. But in the derivation of the resonant spectrum method formulae given in the Appendix, a thin electrode approximation is used. The errors caused by this approximation may be significant for high frequency resonators in which the thickness of the electrodes is comparable with the thickness of the piezoelectric film. Therefore, it is necessary to investigate the available range of the electrode thickness limitation and the errors caused by the electrodes. Fig. 7 shows the SPRF and $k_{\text{eff}}^2(m)$ distributions for various electrode thicknesses in a ZnO/fused quartz composite resonator as Sample I. It can be seen that the thicker the electrode, the greater the $k_{\text{eff}}^2(m)$. These results are qualitatively coincident with (15). Table IV lists the simulation results for ρ, V, and k_t^2 for various electrode thicknesses. It is shown that the errors of the three parameters increase with the increase of the electrode thickness. When the thickness of the aluminum electrodes is within 10% of the ZnO film, the error is less than 5%, which is quite acceptable. The result has a clear mathematical interpretation. As given in the Appendix (A7), an approximation:

$$\tan\gamma_e \approx \gamma_e, \tag{17}$$

is used in deriving the resonant spectrum method, which means the electrodes can be considered as a mass loading. For ZnO/quartz composite resonator with aluminum electrodes as simulated here, V_e is close to V. When the electrode thickness is a tenth of the piezoelectric film thickness:

$$\gamma_e \sim \gamma/10 \approx \pi/10, \tag{18}$$

at the first normal region. The use of approximation of (17) gives an error of 3.4%. With contributions from other approximations, the overall error is about 5%. The condi-

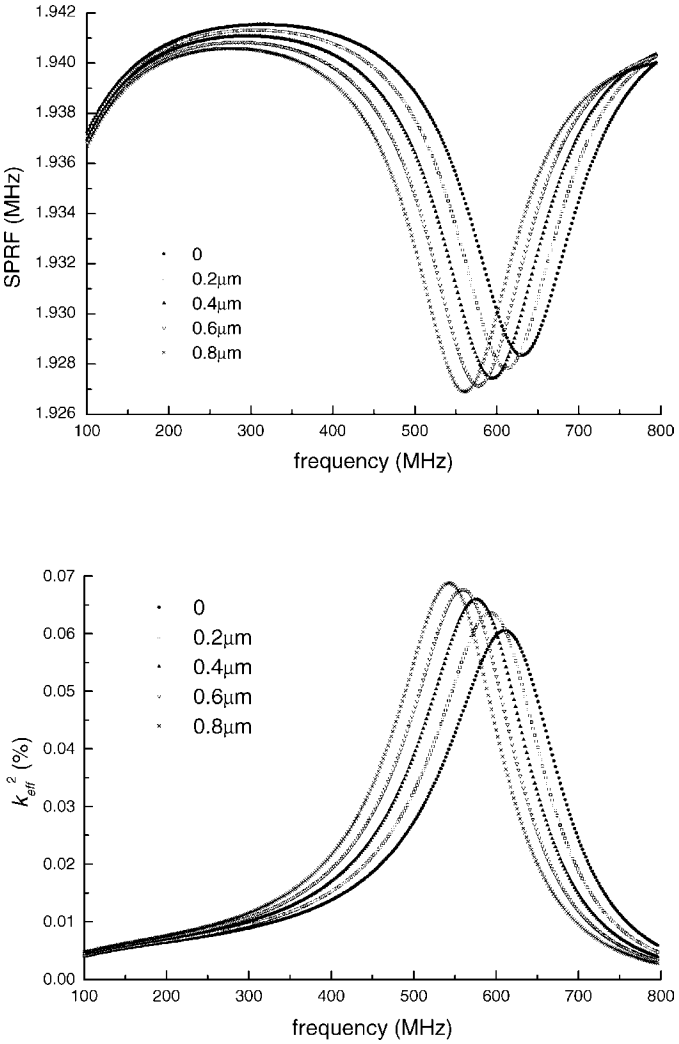

Fig. 7. SPRF (top) and k^2_{eff} (bottom) distribution for various electrode thicknesses in a four-layer ZnO/fused quartz composite resonator.

tion for the electrode thickness being a tenth of the piezoelectric film thickness can be used as a rough criterion to achieve good accuracy.

As a further comparison, we use the resonant spectrum method formulae with the electrode effect ignored [8]. Let $l_{e1} = l_{e2} = 0$, (15) becomes:

$$k_t^2 = \left(1 + \frac{\rho_{sb} l_{sb}}{\rho l}\right) k^2_{\text{eff}}(m_N + 1). \tag{19}$$

For the 0.4-μm electrode case in Table IV, k_t^2 will be 7.83%, and the error will be 7.74% when other parameters use the input value in Table I. If the velocity and density use the simulation results in Table III, the error of k_t^2 will be 10%. When taking the electrode effect into account and using (15), we find that the error of k_t^2 is only 2.1%. The result shows clearly that effects of the electrode have to be compensated and our modified formulae are effective.

The data given in Table IV shows that the results obtained from (15) seem better than those from (9). This may be caused from the approximation of m_N introducing an opposite error that cancels out part of the error from (9).

VI. Effect of Mechanical Loss

In deriving the parallel and series resonant frequencies determination (2) and (3), from which the formulae for evaluating k_t^2 are derived, all the material parameters are assumed to be real. This means all materials are assumed lossless. For high frequency devices or porous piezoelectric ceramics, however, the losses are significant in determination of the electric input impedance of a resonator, from which the resonant frequencies are calculated. Therefore, it is necessary to investigate the validity of the resonant spectrum method when the materials are lossy, in another word, whether (9) and (10) are available when the resonant frequencies are directly calculated from impedance (1).

The effect of the mechanical losses on evaluating k_t^2 is investigated with numerical simulation by taking the velocity as a complex value. The ratio of the real part to imaginary part of the velocity is referred to as material Q value. Taking different Q values for the piezoelectric film and the substrate, and directly calculating the resonant frequency spectra from the electric impedance of the composite resonator, we evaluated the corresponding $k^2_{\text{eff}}(m_N + 1)$. Because k_t^2 is definitely determined by $k^2_{\text{eff}}(m_N + 1)$ or $k^2_{\text{eff}}(m_T + 1)$ when other material parameters are taken as constants, only the $k^2_{\text{eff}}(m)$ distribution is necessary to be simulated for different loss.

Fig. 8 shows the electric input impedance of the ZnO/SiO_2 composite resonators with different material Q values. In Fig. 8(b) the Q values of the two materials are chosen such that the impedance is close to the experimental result [Fig. 8(a)]. Figs. 8(c) and 8(d) are the cases in which the material Q values are much higher and much lower, respectively. In the high Q case, the imaginary parts of the velocities of the piezoelectric film and the substrate decrease to 1/10 and 1/2 from the nominal values in Fig. 8(b), respectively. In the low Q case, the imaginary parts increase by five times and twice, respectively. It is shown that the resonant amplitude changes significantly. The smaller the propagation losses, the higher the resonant peaks, and vice versa.

The distribution curves of $k^2_{\text{eff}}(m)$ versus the frequency are shown in Fig. 9 for high Q and low Q cases. It is noticed that, although the mechanical losses in the piezoelectric film and substrate have been changed by 50 and 4 times, the distributions of $k^2_{\text{eff}}(m)$ have no significant difference. The value at the first normal region $k^2_{\text{eff}}(m_N + 1)$ changes only 1.6%. Thus, k_t^2 of the piezoelectric film calculated from $k^2_{\text{eff}}(m_N + 1)$ with the resonant spectrum method is insensitive to the mechanical loss for moderate loss piezoelectric films. This behavior is in accordance with Naik *et al.* [4] and the IEEE standard [5].

Other simulations show that, when the loss in the substrate is taken as the nominal value, the 50 times variation of the loss in the piezoelectric film brings a trivial difference to the $k^2_{\text{eff}}(m)$. This is in accordance with the

TABLE IV
METHOD ERRORS FOR VARIOUS ALUMINUM ELECTRODE THICKNESSES IN ZNO/FUSED QUARTZ COMPOSITE RESONATOR.

Electrode thickness	ρ		V		c_{33}^D		k_t^2 (9)		k_t^2 (15)	
	(kg/m^3)	error	(m/s)	error	($10^{10}N/m^2$)	error	(%)	error	(%)	error
0	5654.5	−0.2%	6072.6	0.2%	20.85	0.1%	7.19	−1.1%	7.21	−0.8%
0.2 μm	5625.1	0.7%	6080.6	0.3%	20.80	−0.1%	7.15	−1.7%	7.17	−1.4%
0.4 μm	5544.2	−2.1%	6106.1	0.7%	20.67	−0.8%	7.05	−3.0%	7.12	−2.1%
0.6 μm	5430.2	−4.2%	6154.7	1.5%	20.57	−1.2%	6.88	−5.4%	7.05	−3.0%
0.8 μm	5290.4	−6.6%	6212.2	2.5%	20.42	−2.0%	6.64	−8.7%	6.89	−5.2%

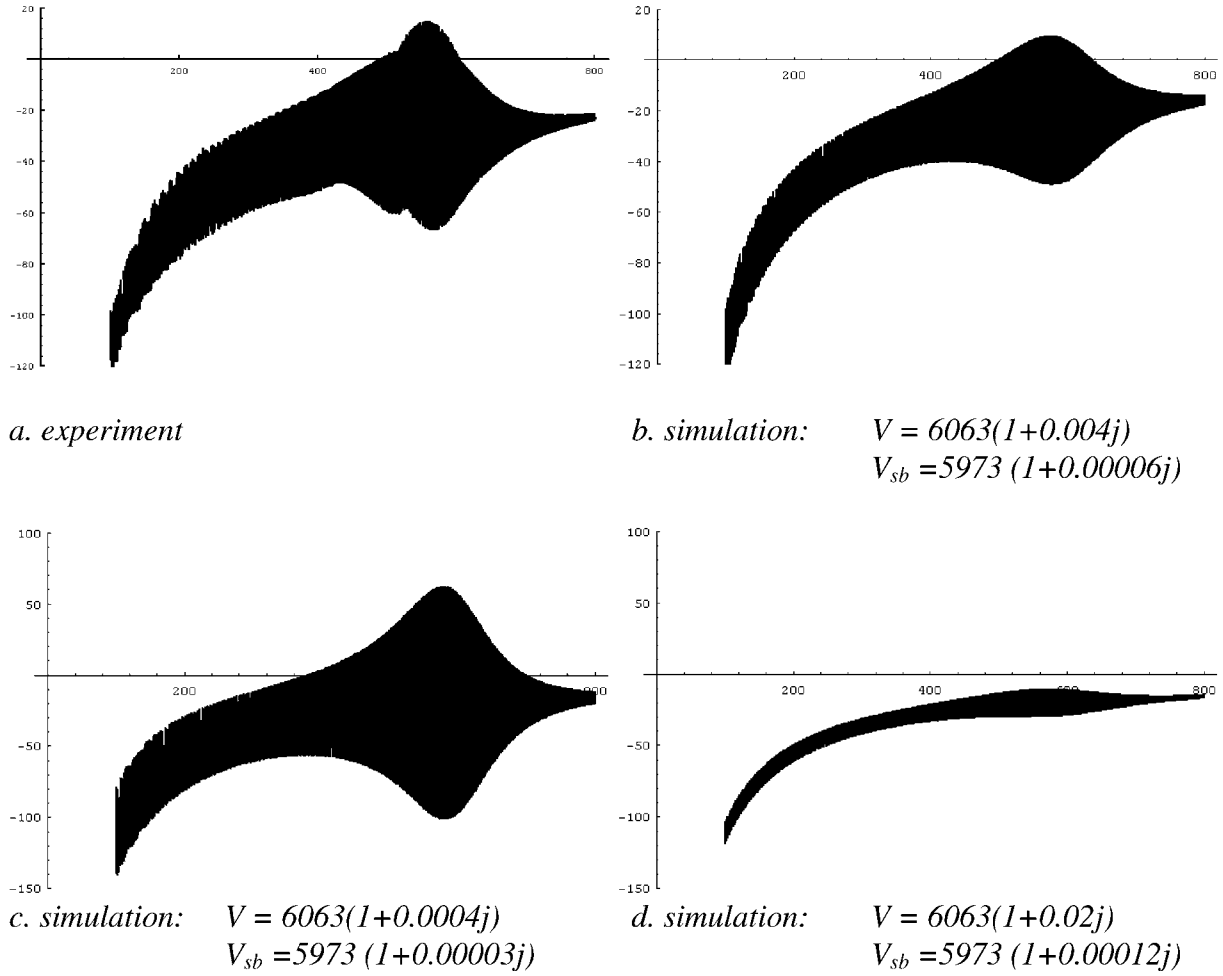

Fig. 8. Imaginary part electric impedances of ZnO/fused quartz resonators with different material mechanical losses showing a significant effect of the loss on the resonant amplitude. Horizontal axes, frequency in MHz; Vertical axes, imaginary part impedance in Ω.

physical nature of a composite resonator that the acoustic wave travels most of the time in the substrate, and the loss of the piezoelectric film has little effect. Because the substrate is usually high quality materials such as fused quartz or silicon, their acoustic losses are fairly constant and will not exceed the variation range in the simulation of Fig. 9. Therefore, the effect of mechanical loss in both the piezoelectric film and the substrate for practical materials may be much less than what have been shown in the simulation Fig. 9. This feature gives further advantages to the resonant spectrum method for keeping good accuracy for a wide range of practical piezoelectric films up to moderate high mechanical loss.

VII. CONCLUSIONS

The principles of a direct measurement method for piezoelectric film, named as the resonant spectrum method, are presented briefly. After knowing the resonant spectrum of a composite resonator, three major parameters of piezoelectric films (i.e., the electromechanical cou-

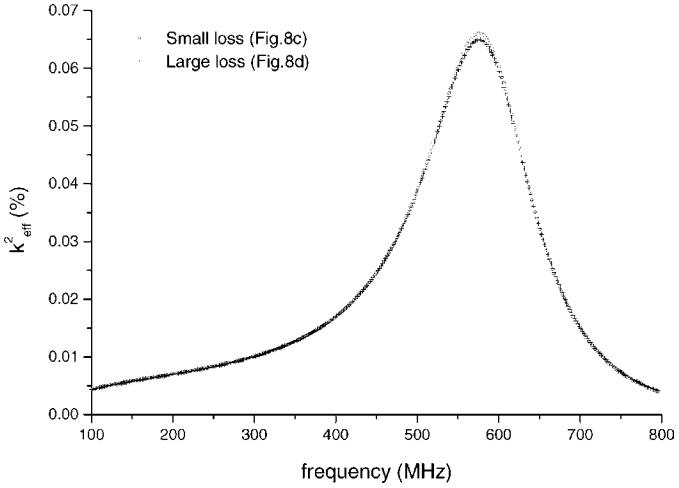

Fig. 9. k^2_{eff} distribution of ZnO/fused quartz resonators for different material mechanical losses showing the small effect of the loss on the k^2_{eff}.

pling coefficient), the elastic constant and the density can be evaluated by a set of explicit formulae. It has been found that the acoustic impedance ratio of the piezoelectric film and the substrate dominates the SPRF and k^2_{eff} distributions. For the soft substrate case where $z_{sb} < 1$, Δf_N of the SPRF is the minimum and Δf_T is the maximum. The k^2_{eff} has maximum at the first normal region and (9) or (15) should be used to calculate the k_t^2. Contrarily, for the hard substrate case where $z_{sb} > 1$, Δf_N of the SPRF is the maximum and Δf_T is the minimum. The k^2_{eff} has maximum at the first transition region and (10) or (16) should be used to calculate the k_t^2.

Measurement on two samples of ZnO/fused quartz resonators was carried out, and the results are reasonable. Simulation results show that, for thin electrode in which the electrode can be considered as mass loading, the effects introduced by the electrode can be compensated by the modified formulae derived in this paper. As a result, the errors are less than 5% if the thickness of the electrode is not more than 10% of that of the piezoelectric film. The effect of the mechanical losses in the substrate and piezoelectric film on the accuracy of this method has been investigated by numerical simulation, and it is shown that the effect is small for practical composite resonators.

This method can find wide application in piezoelectric film characterization. An obvious advantage of the resonant spectrum method is the "directness". Usually, the parameters of the piezoelectric films are determined by fitting the data from their electric characteristic measurements, for example, the electric input impedance. This method, also based on the electric impedance measurement, can calculate three parameters directly. Another advantage of the method is that only the distributions of resonant frequencies are of interest. Therefore, the calibration of the measurement system is not critical, even though the accuracy of the calibration makes a considerable difference in the measurement of electric impedance. This feature is convenient for some applications in which accurate calibration is difficult. In addition, the k_t^2 deduced by this method is not sensitive to the loss of the piezoelectric film, this implies that this method can apply to moderate high loss, low Q factor piezoelectric film characterization.

The formulae presented in this paper are also useful for designing overmoded resonator filter [12], [13]. The bandwidth of such filter is mainly determined by the effective electromechanical coupling coefficient k^2_{eff}. By knowing the material electromechanical coupling coefficient k_t^2, the k^2_{eff} value of the mode in normal or transition region can be evaluated directly from the formulae given in Section II. A suitable k^2_{eff} value can be optimized by choosing proper material parameters and thickness of the composite resonator.

There are some limits on this method. The electrodes of the resonator have to be very thin compared to the piezoelectric film. This limits the application of this method to a frequency range under 1 GHz. In addition, there have to be enough resonant modes in one period of SPRF to use the approximation (15) and (16). This requires a large thickness ratio of the substrate to the piezoelectric film. As a result, the inaccuracy of the substrate parameters has more impact on the accuracy of the resonant spectrum method.

Appendix A
Derivation of the Resonant Spectrum Method

A. The Electric Input Impedance of a Composite Resonator

The acoustic impedance of each layer in a composite resonator can be described using Sittig's matrix presentation [14]. A schematic of a four-layer composite resonator is shown in Fig. 10.

The acoustic impedance of the top electrode, presenting at the left side of the piezoelectric layer, is given by:

$$Z_1 = \frac{F_0}{u_0} = jZ_{e1}\tan\gamma_{e1}, \tag{A1}$$

where F and u represent force and displacement velocity, respectively, $Z_{e1} = S\rho_{e1}V_{e1}$ is the acoustic impedance of the top electrode, $\gamma_{e1} = \omega l_{e1}/V_{e1}$ is the phase delay in the top electrode.

The acoustic impedance of the middle electrode and the substrate, presenting at the right side of the piezoelectric layer, is given by:

$$Z_2 = \frac{F_1}{u_1} = j\frac{Z_{sb}\tan\gamma_{sb} + Z_{e2}\tan\gamma_{e2}}{1-(Z_{sb}/Z_{e2})\tan\gamma_{e2}\tan\gamma_{sb}}, \tag{A2}$$

where $\gamma_{e2} = \omega l_{e2}/V_{e2}$, $\gamma_{sb} = \omega l_{sb}/V_{sb}$ are the phase delay in the middle electrode and the substrate, respectively; $Z_{e2} = S\rho_{e2}V_{e2}$, $Z_{sb} = S\rho_{sb}V_{sb}$ are the acoustic impedances, ρ_{e2}, ρ_{sb} are the densities, V_{e2}, V_{sb} are the velocity of this two layers, respectively.

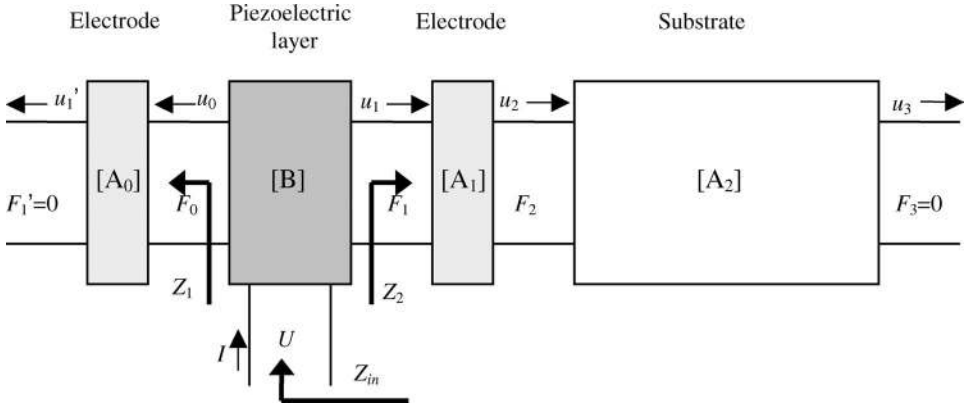

Fig. 10. The matrix model to derive the electric input impedance of a four-layer composite resonator.

The electric input impedance of such a four-layer composite resonator is given by:

$$Z_{in} = \frac{U}{I} = \frac{1}{j\omega C_0}\left[1 - \frac{k_t^2}{\gamma}\frac{(z_1+z_2)\sin\gamma + j2(1-\cos\gamma)}{(z_1+z_2)\cos\gamma + j(1+z_1z_2)\sin\gamma}\right], \tag{A3}$$

where $z_1 = Z_1/Z_0$ and $z_2 = Z_2/Z_0$ are the normalized acoustic impedance of the top electrode layer and the middle electrode/substrate combination.

B. The First Normal Region. Δf_N and k_t^2

Parallel resonances correspond to maximums of the resistance of a composite resonator. If we ignore the imaginary parts of material parameters, parallel resonances correspond infinite impedance $Z_{in} \to \infty$, which gives a determinative equation for the parallel resonant frequencies:

$$(z_1+z_2)\cos\gamma + j(1+z_1z_2)\sin\gamma = 0. \tag{A4}$$

At the center of the first normal region, the $m_N + 1$ order resonant mode corresponds to:

$$\gamma \approx \pi, \qquad \gamma_{sb} \approx m_N\pi, \tag{A5}$$

where m_N is the mode order of the bare substrate plate resonator at the center of the first normal region. So we have approximate expressions as:

$$\tan\gamma \approx \gamma - \pi, \qquad \tan\gamma_{sb} \approx \gamma_{sb} - m_N\pi. \tag{A6}$$

Because the electrodes usually are much thinner than the piezoelectric film, this means $\gamma_{e1} \ll 1$ and $\gamma_{e2} \ll 1$ at the first normal region, thus:

$$\tan\gamma_{e1} \approx \gamma_{e1}, \qquad \tan\gamma_{e2} \approx \gamma_{e2}. \tag{A7}$$

Therefore,

$$z_1 \approx j\frac{Z_{e1}}{Z_0}\gamma_{e1} = jz_{e1}\gamma_{e1}, \tag{A8}$$

and

$$z_2 \approx j\frac{z_{sb}(\gamma - m_N\pi) + z_{e2}\gamma_{e2}}{1 - (z_{sb}/z_{e2})(\gamma_{sb} - m_N\pi)\gamma_{e2}} \approx j\left[z_{sb}(\gamma - m_N\pi) + z_{e2}\gamma_{e2}\right]. \tag{A9}$$

Substitute approximations (A5)–(A9) into (A4), we get (A10) (see next page).

The $(m_N + 1)$-order parallel resonant frequency of the composite resonator is:

$$f_P(m_N+1) = \frac{(m_N z_{sb} + 1)}{2\left(\frac{z_{e1}l_{e1}}{V_{e1}} + \frac{z_{sb}l_{sb}}{V_{sb}} + \frac{z_{e2}l_{e2}}{V_{e2}} + \frac{l}{V}\right)}. \tag{A11}$$

The space between two parallel resonant frequencies at the first normal region is:

$$\begin{aligned}\Delta f_N &= \frac{1}{2}\frac{z_{sb}}{\frac{z_{e1}l_{e1}}{V_{e1}} + \frac{z_{sb}l_{sb}}{V_{sb}} + \frac{z_{e2}l_{e2}}{V_{e2}} + \frac{l}{V}} \\ &= \frac{1}{2}\frac{\rho_{sb}V_{sb}}{\rho_{e1}l_{e1} + \rho_{sb}l_{sb} + \rho_{e2}l_{e2} + \rho l} \\ &= \Delta f_0\left(1 + \frac{\rho_{e1}l_{e1} + \rho_{e2}l_{e2} + \rho l}{\rho_{sb}l_{sb}}\right)^{-1},\end{aligned} \tag{A12}$$

where $\Delta f_0 = \frac{V_{sb}}{2l_{sb}}$ is the parallel resonance frequency spacing of a bare substrate plate.

On the other hand, the series resonant frequencies (3) give:

$$k_t^2 = \frac{\gamma[(z_1+z_2) + j(1+z_1z_2)\tan\gamma]}{(z_1+z_2)\tan\gamma + 2j(\sec\gamma - 1)}, \tag{A13}$$

at series resonant frequencies. As proven before, both z_1 and z_2 are first-order small quantities at a resonance in the first normal region. Therefore, $z_1z_2 \ll 1$ and $(z_1+z_2)(\gamma - \pi) \ll 1$. Ignoring these second-order small quantities, we get an approximate expression for k_t^2 given in (A14) (see next page).

Substitute (A11) into the (A14) to get (A15) (see next page).

If we introduce an effective coupling coefficient k_{eff}^2 as:

$$k_{\text{eff}}^2 = \frac{\pi^2}{4}\frac{f_s}{f_p}\left(\frac{f_p - f_s}{f_p}\right), \tag{A16}$$

$$\begin{aligned}&(jz_{e1}\gamma_{e1} + j[z_{sb}(\gamma - m_N\pi) + z_{e2}\gamma_{e2}])\\&+ j(1 + jz_{e1}\gamma_{e1}\cdot j[z_{sb}(\gamma - m_N\pi) + z_{e2}\gamma_{e2}])(\gamma - \pi) = 0,\\&\left[z_{e1}\frac{2\pi f l_{e1}}{V_{e1}} + z_{sb}\left(\frac{2\pi f l_{sb}}{V_{sb}} - m_N\pi\right) + z_{e2}\frac{2\pi f l_{e2}}{V_{e2}}\right]\\&+ \left\{1 - z_{e1}\frac{2\pi f l_{e1}}{V_{e1}}\left[z_{sb}\left(\frac{2\pi f l_{sb}}{V_{sb}} - m_N\pi\right) + z_{e2}\frac{2\pi f l_{e2}}{V_{e2}}\right]\right\}\left(\frac{2\pi f l}{V} - \pi\right) = 0\end{aligned} \tag{A10}$$

$$\begin{aligned}k_t^2 &= \frac{\gamma}{-4j}[(z_1 + z_2) + j(\gamma - \pi)]\\&= \frac{1}{-4}\frac{2\pi f_s l}{V}\left[2\pi f_s\left(z_{e1}\frac{l_{e1}}{V_{e1}} + z_{sb}\frac{l_{sb}}{V_{sb}} + z_{e2}\frac{l_{e2}}{V_{e2}} + \frac{l}{V}\right) - (z_{sb}m_N + 1)\,\pi\right]\end{aligned} \tag{A14}$$

$$\begin{aligned}k_t^2 &= \frac{\pi^2 l}{V} f_s(f_p - f_s)\left(z_{e1}\frac{l_{e1}}{V_{e1}} + z_{sb}\frac{l_{sb}}{V_{sb}} + z_{e2}\frac{l_{e2}}{V_{e2}} + \frac{l}{V}\right)\\&= \frac{\pi^2}{4}\frac{f_s}{f_p}\frac{f_p - f_s}{f_p}\frac{(1 + m_N z_{sb})^2}{\left(1 + \frac{\rho_{e1}l_{e1} + \rho_{e2}l_{e2} + \rho_{sb}l_{sb}}{\rho l}\right)}\end{aligned} \tag{A15}$$

the coupling coefficient k_t^2 can be expressed as:

$$k_t^2 = \frac{(1 + m_N z_{sb})^2}{\left(1 + \frac{\rho_{e1}l_{e1} + \rho_{e2}l_{e2} + \rho_{sb}l_{sb}}{\rho l}\right)}k_{\text{eff}}^2. \tag{A17}$$

In some special cases, the k_t^2 equation can be further simplified. As shown in (A5), m_N is the resonant mode order of the substrate plate at the center of the first normal region. For the case of a four-layer composite resonator, the composite resonator can be considered as a top resonator composed of a piezoelectric film, a top electrode, and part of a middle electrode deposited on a composite substrate composed of the other part of the middle electrode and a substrate plate. As an approximation, we split half of the middle electrode into the top resonator and the other half into the composite substrate. The center frequency of the first normal region corresponds to the resonant frequency of the top resonator:

$$f_c = \frac{V}{2\left(l + \rho_{e1}l_{e1}/\rho + \frac{1}{2}\rho_{e2}l_{e2}/\rho\right)}. \tag{A18}$$

The fundamental resonant frequency of the composite substrate is:

$$f_{sb} = \frac{V_{sb}}{\left(l_{sb} + \frac{1}{2}\rho_{e2}l_{e2}/\rho_{sb}\right)}. \tag{A19}$$

We define R as the ratio of resonant frequency of the top resonator to the fundamental resonant frequency of the composite substrate:

$$R = \frac{f_c}{f_{sb}} = \frac{V\left(l_{sb} + \frac{1}{2}\rho_{e2}l_{e2}/\rho_{sb}\right)}{V_{sb}\left(l + \rho_{e1}l_{e1}/\rho + \frac{1}{2}\rho_{e2}l_{e2}/\rho\right)}. \tag{A20}$$

m_N is the value of R rounded to the nearest integer:

$$m_N = \text{the nearest integer of } R. \tag{A21}$$

It should be noted that the resonant mode order of the composite resonator at the center of the first normal region, is $m_N + 1$, rather than m_N.

If R is close to an integer, or is large enough that the fraction part can be ignored, $m_N \approx R$:

$$1 + m_N z_{sb} = \frac{\rho l + \rho_{e1}l_{e1} + \rho_{e2}l_{e2} + \rho_{sb}l_{sb}}{\rho l + \rho_{e1}l_{e1} + \frac{1}{2}\rho_{e2}l_{e2}}. \tag{A22}$$

Substitute (A22) into (A17), we get a simplified expression for the electromechanical coupling coefficient:

$$k_t^2 = \frac{\rho l(\rho l + \rho_{e1}l_{e1} + \rho_{e2}l_{e2} + \rho_{sb}l_{sb})}{(\rho l + \rho_{e1}l_{e1} + \frac{1}{2}\rho_{e2}l_{e2})^2}k_{\text{eff}}^2(m_N + 1). \tag{A23}$$

C. The First Transition Region, Δf_T and k_t^2

The first transition region occurs where $\gamma = \pi/2$. Because, in a resonator, the total phase delay has to be an integer multiplication of π, the phase shift of the substrate will yield another $\pi/2$. We assume that:

$$\gamma = \pi/2 + \Delta, \qquad \gamma_{sb} = (m_T + 1/2)\pi + \delta, \tag{A24}$$

where m_T is the mode order of the bare substrate plate near the center of the first transition region, Δ and δ are small quantities. Therefore, we get approximate expressions at the first transition region as:

$$\sin\gamma \approx 1, \quad \cos\gamma \approx -\Delta, \quad \tan\gamma_{sb} \approx -1/\delta. \tag{A25}$$

By taking these approximations into the expression of z_2, we get:

$$\begin{aligned} z_2 &= \frac{j}{Z_0}\frac{Z_{sb}\tan\gamma_{sb} + Z_{e2}\tan\gamma_{e2}}{1-(Z_{sb}/Z_{e2})\tan\gamma_{sb}\tan\gamma_{e2}} \\ &\approx j\frac{z_{sb}\frac{1}{-\delta} + z_{e2}\gamma_{e2}}{1+\frac{z_{sb}}{z_{e2}}\frac{\gamma_{e2}}{\delta}} \\ &\approx -j\left(\frac{\delta}{z_{sb}} + \frac{\gamma_{e2}}{z_{e2}}\right)^{-1}. \end{aligned} \tag{A26}$$

Take the approximations (A8), (A25), and (A26) into the parallel resonance frequency (A4), we get:

$$\begin{aligned} &\left(jz_{e1}\gamma_{e1} - j\left(\frac{\delta}{z_{sb}} + \frac{\gamma_{e2}}{z_{e2}}\right)^{-1}\right)\cdot(-\Delta) \\ &+ j\left(1 - j(jz_{e1}\gamma_{e1})\left(\frac{\delta}{z_{sb}} + \frac{\gamma_{e2}}{z_{e2}}\right)^{-1}\right)\cdot 1 = 0. \end{aligned}$$

In the first bracket, the first term is a small quantity, and the second term is a large quantity. As an approximation, we ignore the first term and after some simplification, we may get:

$$\Delta + \frac{\delta}{z_{sb}} + \frac{\gamma_{e2}}{z_{e2}} + z_{e1}\gamma_{e1} = 0. \tag{A27}$$

Therefore, we can get the parallel resonant frequency at the first transition region:

$$f_p(m_T+1) = \frac{1}{2z_{sb}}\frac{m_T + 1/2 + z_{sb}/2}{\left(\frac{l}{V} + \frac{l_{sb}}{z_{sb}V_{sb}} + \frac{l_{e2}}{z_{e2}V_{e2}} + z_{e1}\frac{l_{e1}}{V_{e1}}\right)}. \tag{A28}$$

So the spacing of the parallel resonance frequencies at the first transition region is:

$$\begin{aligned} \Delta f_T &= \frac{1}{2z_{sb}}\frac{1}{\left(\frac{l}{V} + \frac{l_{sb}}{z_{sb}V_{sb}} + \frac{l_{e2}}{z_{e2}V_{e2}} + z_{e1}\frac{l_{e1}}{V_{e1}}\right)} \\ &= \Delta f_0\left(1 + \frac{\rho_{sb}V_{sb}^2}{\rho V^2}\frac{l}{l_{sb}} + \frac{\rho_{sb}V_{sb}^2}{\rho_{e2}V_{e2}^2}\frac{l_{e2}}{l_{sb}} + \frac{\rho_{sb}\rho_{e1}V_{sb}^2}{\rho^2V^2}\frac{l_{e1}}{l_{sb}}\right)^{-1}. \end{aligned} \tag{A29}$$

As at the first normal region, the series resonance frequencies at the first transition region are determined by (3). Since:

$$z_2 \approx -j\left(\frac{\delta}{z_{sb}} + \frac{\gamma_{e2}}{z_{e2}}\right)^{-1} \gg 1 \text{ and } z_1 = jz_{e1}\gamma_{e1} \ll 1, \tag{A30}$$

(3) at the first transition region can be expressed as:

$$z_2(-\Delta) + j(1 + z_1z_2) = \frac{k_t^2}{\gamma}\left[z_2 + j2(1+\Delta)\right]. \tag{A31}$$

Therefore, k_t^2 can be calculated from:

$$\begin{aligned} k_t^2 &= \gamma\frac{z_2(-\Delta) + j(1+z_1z_2)}{[z_2 + j2(1+\Delta)]} \\ &= \gamma\frac{z_2(-\Delta) + j(1+z_1z_2)}{z_2\Gamma} \\ &= \frac{[1 + (2m_T+1)/z_{sb}]^2}{1 + \frac{V}{l}\left(\frac{l_{sb}}{z_{sb}V_{sb}} + \frac{l_{e2}}{z_{e2}V_{e2}} + z_{e1}\frac{l_{e1}}{V_{e1}}\right)}\frac{k_{\text{eff}}^2}{\Gamma}. \end{aligned} \tag{A32}$$

Γ is a correction factor, which is in the order of unity:

$$\begin{aligned} \Gamma =& 1 + 2j\frac{(1+\Delta)}{z_2} \\ =& 1 - 2\rho_0V\left(1 + \frac{2\pi f_s l}{v} - \frac{\pi}{2}\right) \\ & \left(\frac{2\pi f_s l}{\rho_{sb}V_{sb}^2} - \frac{(m_T+1/2)\pi}{\rho_{sb}V_{sb}} + \frac{2\pi f_s l_{e2}}{\rho_{e2}V_{e2}^2}\right). \end{aligned} \tag{A33}$$

This correction factor stands for the difference between the first transition region center and the (m_T+1) mode series resonance frequency.

Again, as at the first normal region, m_T is the value of $(R-1)/2$ rounded to the nearest integer:

$$M_T = \text{the nearest integer of } \left(\frac{R-1}{2}\right). \tag{A34}$$

When R is close to an odd integer or is large enough, $m_T \approx \frac{R-1}{2}$, see (A35) (see next page).

Because the electrodes usually are very thin compared to the substrate, the electromechanical coupling coefficient expression at the first transition region can be simplified by substituting (A35) into (A32) to get (A36) (see next page).

It has to be noted that, even in the case that R is an odd integer or large enough, $\Gamma \approx 1$ is not necessarily hold.

Acknowledgment

The authors would like to thank Dr. F. S. Hickernell at Motorola for providing the samples. Y. Zhang is very grateful to Concordia University for the Concordia University Fellowship award.

References

[1] L. Zuo, M. Sayer, and C.-K. Jen, "Sol-gel fabricated thick piezoelectric ultrasonic transducers for potential applications in industrial material processes," in *Proc. IEEE Ultrason. Symp.*, 1997, pp. 1007–1011.

$$1+(2m_T+1)/z_{sb} \approx 1+R/z_{sb} = \frac{1+\frac{\rho_{e1}l_{e1}}{\rho l}+\frac{\rho V^2}{\rho_{sb}V_{sb}^2}\frac{l_{sb}}{l}+\frac{1}{2}\left(\frac{\rho^2V^2}{\rho_{sb}^2V_{sb}^2}+1\right)\frac{\rho_{e2}l_{e2}}{\rho l}}{1+\frac{\rho_{e1}l_{e1}}{\rho l}+\frac{1}{2}\frac{\rho_{e2}l_{e2}}{\rho l}}. \tag{A35}$$

$$k_t^2 = \frac{1+\frac{\rho_{e1}l_{e1}}{\rho l}+\frac{\rho V^2}{\rho_{sb}V_{sb}^2}\frac{l_{sb}}{l}+\frac{1}{2}\left(\frac{\rho^2V^2}{\rho_{sb}^2V_{sb}^2}+1\right)\frac{\rho_{e2}l_{e2}}{\rho l}}{\left(1+\frac{\rho_{e1}l_{e1}}{\rho l}+\frac{1}{2}\frac{\rho_{e2}l_{e2}}{\rho l}\right)^2}\frac{k_{\text{eff}}^2(m_T+1)}{\Gamma}. \tag{A36}$$

[2] R. M. Malbon, D. J. Walsh, and D. K. Winslow, "Zinc-oxide film microwave acoustic transducers," *Appl. Phys. Lett.*, vol. 10, no. 1, pp. 9–10, 1967.

[3] F. S. Hickernell, "Measurement techniques for evaluating piezoelectric thin films," in *Proc. IEEE Ultrason. Symp.*, 1996, pp. 235–242.

[4] B. S. Naik, J. J. Lutsky, R. Rief, and C. D. Sodini, "Electromechanical coupling constant extraction of thin-film piezoelectric materials using a bulk acoustic wave resonator," *IEEE Trans. Ultrason., Ferroelect., Freq. Contr.*, vol. 45, no. 1, pp. 257–263, 1998.

[5] "IEEE Standard on Piezoelectricity (ANSI/IEEE Std. 176-1987)," *IEEE Trans. Ultrason., Ferroelect., Freq. Contr.*, vol. 43, no. 5, pp. 719–772, 1996.

[6] A. J. Bahr and I. N. Court, "Determination of the electromechanical coupling coefficient of thin-film cadmium sulphide," *J. Appl. Phys.*, vol. 39, no. 6, pp. 2863–2868, 1968.

[7] A. H. Meitzler and E. K. Sittig, "Characterization of piezoelectric transducers used in ultrasonic devices operating above 0.1 GHz," *J. Appl. Phys.*, vol. 40, no. 11, pp. 4341–4352, 1969.

[8] Z. Wang, Y. Zhang, and J. D. N. Cheeke, "Characterization of electromechanical coupling coefficient of piezoelectric film using composite resonators," *IEEE Trans. Ultrason., Ferroelect., Freq. Contr.*, vol. 46, no. 5, pp. 1327–1330, 1999.

[9] Y. Zhang, Z. Wang, J. D. N. Cheeke, and F. S. Hickernell, "Direct characterization of ZnO films in composite resonators with the resonance spectrum method," in *Proc. IEEE Ultrason. Symp.*, 1999, pp. 991–994.

[10] F. S. Hickernell, personal communication, 1998.

[11] B. A. Auld, "Appendix 2: Properties of materials," in *Acoustic Fields and Waves in Solids*. vol. 1, New York: Wiley, 1973.

[12] K. M. Lakin, G. R. Kline, and K. T. McCarron, "High-Q microwave acoustic resonators and filters," *IEEE Trans. Microwave Theory Tech.*, vol. 41, no. 12, pp. 2139–2145, 1993.

[13] Y. Zhang, "Resonant spectrum method to characterize piezoelectric films in composite resonators," Ph.D. dissertation, Concordia University, Montreal, Quebec, Feb. 2002.

[14] E. K. Sittig, "Design and technology of piezoelectric transducers for frequencies above 100 MHz," *Physical Acoustics,* vol. IX, W. P. Mason and R. N. Thurston, Eds. New York: Academic, pp. 221–275, 1972.

Yuxing Zhang was born in Changzhou, China, in 1964. He received the B.Eng. degree in electric engineering from the University of Science and Technology of China, Hefei, China, in 1987; the M.S. degree in acoustics from the Institute of Acoustics, Chinese Academy of Sciences, Beijing, China, in 1991; and the Ph.D. in applied physics from Concordia University, Montreal, Canada, in 2002.

From 1991 to 1996, he was a research assistant then research fellow with the Ultrasonic Electronics Laboratory, the Institute of Acoustics, Chinese Academy of Sciences, where he was involved in research and design of SAW sensors, SAW programmable matched filters, SAW dispersive delay lines, and SAW Chirp-Z-Transform spectrometers. From 1997 to 2002, he was a doctoral student (later part-time) at the Physics Department of Concordia University, where he worked on development of SAW sensors and characterization of piezoelectric films.

Since 1999, Dr. Zhang has been with the Microelectronics Group and the Wireless Technology Lab, Nortel Networks Inc., Ottawa, Canada. His current interests are on design of SAW filters and radio frequency integrated circuits, and their applications in wireless systems.

Zuoqing Wang received the B.S. and the M.S. degrees from the Department of Physics, Nanjing University, Nanjing, China, in 1962 and 1965, respectively. From 1966 to 1988, he worked on microwave acoustics, acousto-optical interactions and their applications, piezoelectric transducer analysis, and surface acoustic wave devices as an Associate Researcher and Associate Research Professor at the Institute of Acoustics, Chinese Academy of Sciences, Beijing, China. From September 1988 to January 2001, his research was involved in acoustic sensors, Lamb-waves propagating in multilayer structures, circumferential waves, and piezoelectric film characterization as a visiting scientist at the Department of Electrical Engineering in McGill University, Montreal, Quebec, the Department of Physics in Sherbrooke University, Sherbrooke, Quebec, and the Department of Physics in Concordia University, Montreal, Quebec.

Since March 2001, Dr. Wang has been engaged in research on quartz crystal resonator technologies as a senior researcher in TXC Corporation, Taiwan, R.O. China.

J. David N. Cheeke (A'87–SM'91) received the Bachelors and the Masters degree in Engineering Physics from UBC, Vancouver, British Colombia, in 1959 and 1961, respectively, followed by the Ph.D. in Low Temperature Physics from Nottingham University, England, in 1965. He then joined the Low Temperature Laboratory, CNRS Grenoble, France, and was also a professor at the Universite de Grenoble, France. In 1975 he moved to the Universite de Sherbrooke, Sherbrooke, Quebec, where he set up an ultrasonics laboratory specializing in physical acoustics, acoustic microscopy, and acoustic sensors. In 1990 he joined the Physics Department at Concordia University, Montreal, Quebec, where he is head of an ultrasonics laboratory and was Chair of the Department from 1992 to 2000. He has published over 120 papers on various aspects of ultrasonics. He is a senior member of the IEEE and an Associate Editor of the *IEEE Transactions on Ultrasonics, Ferroelectrics and Frequency Control*.